Stoichiometry of 7-ethoxycoumarin metabolism by cytochrome P450 2B1 wild-type and five active-site mutants

Xiaojun Fang*, Yasuna Kobayashi, James R. Halpert

Department of Pharmacology and Toxicology, College of Pharmacy, The University of Arizona, Tucson, AZ 85721, USA

Received 28 April 1997; revised version received 4 September 1997

Abstract Recombinant P450 2B1 wild-type and the active-site mutants I114V, F206L, V363A, V363L, and G478S were purified and studied. The efficiency of coupling of reducing equivalents to 7-hydroxycoumarin formation was decreased for all the mutants except I114V. Uncoupling to H_2O was increased for F206L, V363A, and G478S, decreased for V363L, and unchanged for I114V. Uncoupling to H_2O_2 was increased for V363L and decreased for I114V, F206L, and V363A. The findings from this study provide firm biochemical evidence that residues 206, 363, and 478 comprise part of the substrate binding site of P450 2B1.

Key words: Stoichiometry; Cytochrome P450 2B1; Active-site mutant; Uncoupling; 7-Ethoxycoumarin; Hydrogen peroxide

1. Introduction

The cytochrome P450 (P450) superfamily is responsible for the oxidation of a wide range of drugs, carcinogens, environmental pollutants, and other xenobiotics in species ranging from human to bacteria. Any given P450 enzyme usually has the ability to metabolize a number of different substrates, and different P450s often exhibit overlapping specificities [1]. Identifying the structural determinants of substrate specificity and inhibitor selectivity of P450 2B forms from various species including rat [2–6], rabbit [7,8], and dog [9–11] has been a major interest of this laboratory in recent years. Site-directed mutagenesis studies have shown that residues 114, 206, 290, 294, 302, 363, 367, and 478 in P450 2B enzymes determine the substrate specificity and regio- or stereoselectivity and suggest that these residues are found within substrate recognition sites [2–6,11–14]. These residues have counterparts in active-site residues in mammalian P450 2A and 2C enzymes [15] and in bacterial P450s such as P450 101 and 102 [12,16,17].

Recent studies of P450 101 mutants have revealed interesting correlations between the identity and location of key residues and the efficiency of coupling of pyridine nucleotide derived reducing equivalents to product formation [16,17]. With the preferred substrate camphor, P450 101 yields 1 mol of product for each mol of NADH consumed [18,19], whereas uncoupling is observed during the metabolism of other substrates such as ethylbenzene [16]. The cytochrome P450 catalytic cycle is complex and consists of at least seven discrete steps (Fig. 1). Uncoupling occurs in the reaction cycle at three branch points marked by substrate-bound oxy-ferrous ($[FeO_2]^{2+}$-RH), peroxy-ferric ($[FeO_2H]^{2+}$-RH), and iron-oxo ($[FeO]^{3+}$-RH) intermediates, yielding superoxide, hydrogen peroxide, and excess water, respectively. The stoichiometry of mammalian cytochrome P450 catalyzed reactions has been studied both in microsomes and in reconstituted systems [20,21], and uncoupling at one or more of the three branch points is common [20,22]. Only limited information is available, however, on the role of individual residues in determining coupling efficiency of mammalian P450s. Docking of 7-ethoxycoumarin in the active pocket of a 3D model of P450 2B1 [12] has revealed that residues 114, 206, 363, and 478 are all within 5 Å from the substrate (Fig. 2). In order to obtain biochemical evidence for the role of these residues in substrate recognition, we have studied the stoichiometry of the deethylation of ethoxycoumarin by recombinant P450 2B1 wild-type and the mutants I114V, F206L, V363A, V363L, and G478S. As predicted for active-site residues, uncoupling to water was drastically altered in three of the mutants compared with the wild-type enzyme.

2. Materials and methods

2.1. Materials

HEPES was obtained from Calbiochem Corporation (La Jolla, CA), and all other chemicals were obtained from Sigma and were of the highest grade available.

2.2. Purification

P450 2B1 wild-type and the mutants I114V, F206L, V363A, V363L, and G478S were expressed in an *Escherichia coli* system as described [6]. The recombinant enzymes were purified using the previously published two-column protocol (*n*-octylamino Sepharose, hydroxyapatite) [23] with some modifications. The starting material was CHAPS-solubilized membrane preparations representing 50–100 nmol P450/l culture, with a specific P450 content of >1 nmol/mg protein and minimal cytochrome P420 contamination. Refinements to the octylamino Sepharose chromatography procedures included optimizing the amount of P450 applied (5 nmol/ml gel) and eluting with 0.1% Emulgen 913 instead of 0.08% Lubrol. Improved recovery from the hydroxyapatite chromatography was achieved by decreasing the pH of the equilibration and wash buffers from 7.5 to 6.5 and deleting the EDTA.

2.3. Reconstitution and enzymatic reaction

The reconstituted system of P450 2B1 wild-type or mutants contained 2.5 μM P450, 1.9 μM recombinant NADPH-cytochrome P450 reductase [24], and 36 μg/ml DLPC and was equilibrated at room temperature for 10 min prior to use. The molar ratio of P450 reductase:P450 of 0.75 was used in order to minimize the contribution of the reductase alone to hydrogen peroxide formation [22]. The reaction

*Corresponding author. Fax: (1) (520) 626-2466.
E-mail: xfang@ccit.arizona.edu

Abbreviations: P450, cytochrome P450; CHAPS, (3-[(3-cholamidopropyl)-dimethylammonio]-1-propanesulfonate; EDTA, ethylenediaminetetraacetic acid; HEPES, *N*-2-hydroxyethylpiperazine-*N'*-2-ethanesulfonic acid; SDS-PAGE, sodium dodecyl sulfate-polyacrylamide gel electrophoresis; DLPC, dilauroyl-L-3-phosphatidylcholine; reductase, NADPH-cytochrome P450 reductase

PII S0014-5793(97)01173-3

mixture contained 0.095 μM enzyme, 0.071 μM reductase, 300 μM 7-ethoxycoumarin, 15 μM $MgCl_2$, 30 μg/ml DLPC, and 0.05 M HEPES, pH 7.4. The HEPES buffer was freed of iron by passing through a Chelex column. The reaction was initiated by adding 20 mM NADPH to achieve an initial concentration of 0.20 mM and quenched after 10 min by adding 1/10 volume of 0.5 M sulfuric acid. Spectrophotometric measurement of NADPH oxidation and polarographic measurement of oxygen consumption were performed in two parallel reactions derived from the same reaction mixture and thermostated at 37°C from the same water bath. After quenching, H_2O_2 and 7-hydroxycoumarin were measured in both samples.

2.4. 7-Hydroxycoumarin formation

7-Hydroxycoumarin formed in the reaction was quantified using the previously described fluorometric method [25] with some modifications. 100 μl of the quenched reaction mixture was extracted with 1.5 ml of chloroform; then 1.0 ml of 30 mM sodium borate was used to extract the product from 0.6 ml of the chloroform phase. The concentration of product in the borate solution was determined from its fluorescence recorded on a Hitachi F-2000 fluorescence spectrophotometer using excitation and emission wavelengths of 366 and 454 nm, respectively. Authentic 7-hydroxycoumarin was quantitatively recovered under the extraction conditions employed.

2.5. NADPH oxidation

The reaction was performed in a spectrophotometric cuvette thermostated at 37°C. Because 7-ethoxycoumarin absorbs strongly at 340 nm, reactions were monitored at 362 nm, at which the NADPH vs. 7-ethoxycoumarin difference spectrum shows a peak. The rate of NADPH oxidation was calculated from the corrected absorbance change at 362 nm. The correction was made by subtraction of the absorbance change caused by conversion of 7-ethoxycoumarin to 7-hydroxycoumarin from the spectrophotometrically recorded absorbance change at 362 nm. At 362 nm the molar difference extinction coefficient between 7-hydroxycoumarin and 7-ethoxycoumarin is 4.44 M^{-1} cm^{-1}, whereas the molar extinction coefficient of NADPH is 4.08 M^{-1} cm^{-1}.

2.6. Oxygen consumption

The reaction was performed in a RC-1 respiration cell obtained from Cameron Instrument Company (Port Aransas, TX). The respiration cell was equipped with a Clark-type electrode, a teflon-coated stirring bar, a plunger with a narrow hole in its center for sample delivery, and a water-circulation jacket. The oxygen electrode was connected to an OM 2000 Oxygen Meter obtained from Cameron Instrument Company, and the output from the oxygen meter was recorded on a Curken chart recorder. The oxygen measurements were standardized by two methods: (1) addition of increments of 37°C air-saturated deionized water to air-free nitrogen-saturated water thermostated at 37°C, (2) using two standard solutions: air-saturated water and dithionite solution. Since the slopes of the calibration curves prepared from the above two methods did not differ from each other by more than 1%, the instrument was routinely calibrated by the two-standard method. Under the atmospheric pressure, 686 mm Hg, in our laboratory, the calculated oxygen concentration of deionized water saturated with air at 37°C is 177 μM [26] using the calculated oxygen solubility in pure water 6.73 mg/l at 37°C under 760 mm Hg [27]. The oxygen concentration in the reaction mixture at 37°C was 177 μM, determined from the calibration curve. To initiate a reaction, NADPH was injected to the respiration cell through the narrow central hole with the aid of a micro-syringe. Minor absorption of oxygen from the surroundings through the central hole during the reaction was ignored.

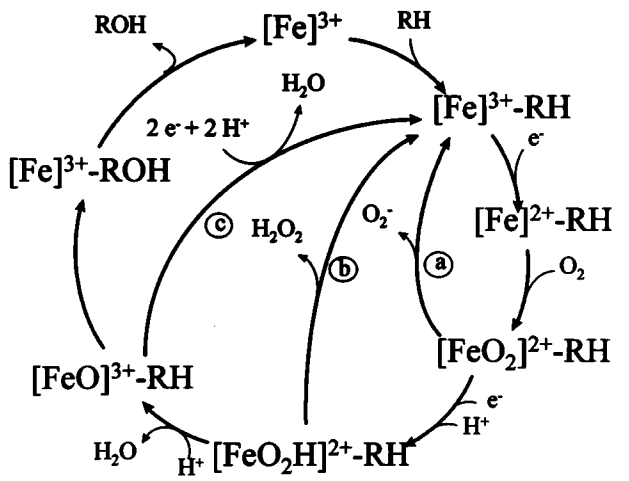

Fig. 1. Cytochrome P450 catalytic cycle. $[Fe]^{3+}$: substrate-free ferric P450. RH: substrate. ROH: hydroxylated product.

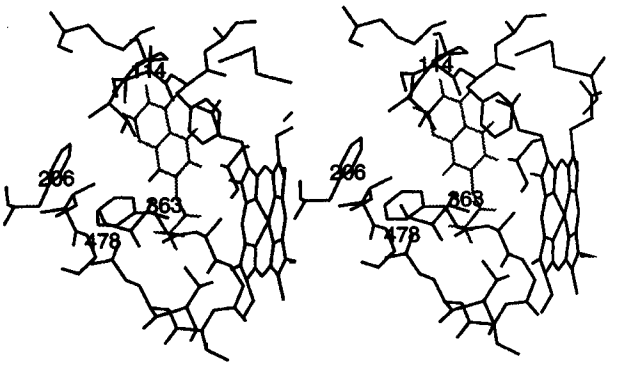

Fig. 2. 7-Ethoxycoumarin docked into the active site of the P450 2B1 model in an orientation allowing for *O*-deethylation. The substrate is shown in gray, with all hydrogens displayed. Key residues 114, 206, 363, and 478 are within 5 Å of 7-ethoxycoumarin.

2.7. Hydrogen peroxide production

The H_2O_2 produced in reactions was determined using the xylenol orange iron(III) colorimetric assay [28] with some modifications. An assay sample was prepared by mixing 100 μl of the quenched reaction mixture with 890 μl of 25 mM sulfuric acid, 10 μl of deionized water, and 17.5 μl of the color developing agent and incubating at room temperature for 1 h. The color developing agent was made prior to use by mixing 1 volume of 20 mM xylenol orange with 2.5 volumes of 20 mM fresh ferrous ammonium sulfate. The calibration curve was prepared from a series of solutions each of which contained 100 μl of the quenched reaction mixture, 890 μl of 25 mM sulfuric acid, 10 μl of H_2O_2 standard solution of different concentrations, and 17.5 μl of the color developing agent. The H_2O_2 standard solutions were prepared by dilution of a 30% H_2O_2 stock solution with deionized water. The exact concentration of H_2O_2 in the stock solution was calculated using the molar extinction coefficient of 43.6 M^{-1} cm^{-1} at 240 nm [28]. Control experiments confirmed that added H_2O_2 was recovered quantitatively from reaction mixtures.

3. Results and discussion

3.1. Enzyme characterization

The purification procedures resulted in wild-type and mutant preparations with a single major band on SDS-PAGE (Fig. 3) and with a specific content of >14 nmol P450/mg protein and $<5\%$ P420. The chromatographic procedures yielded approximately 10–20 nmol purified P450/l culture. Catalytic integrity was confirmed using androstenedione as a substrate. As shown in Fig. 4, the activity of recombinant P450 2B1 was the same as the purified hepatic enzyme. In addition, all mutants showed activities equal to or higher than the membrane preparations (data not shown).

3.2. Stoichiometry of 7-ethoxycoumarin deethylation

The rates of NADPH and oxygen consumption, product formation, and hydrogen peroxide and excess water produc-

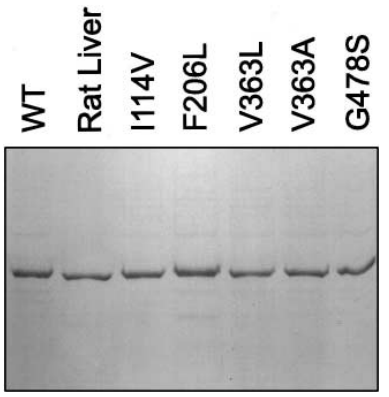

Fig. 3. Coomassie blue-stained SDS-PAGE gel of purified hepatic and recombinant P450 2B1 wild-type and five active-site mutants. Each lane contained 1 μg of protein.

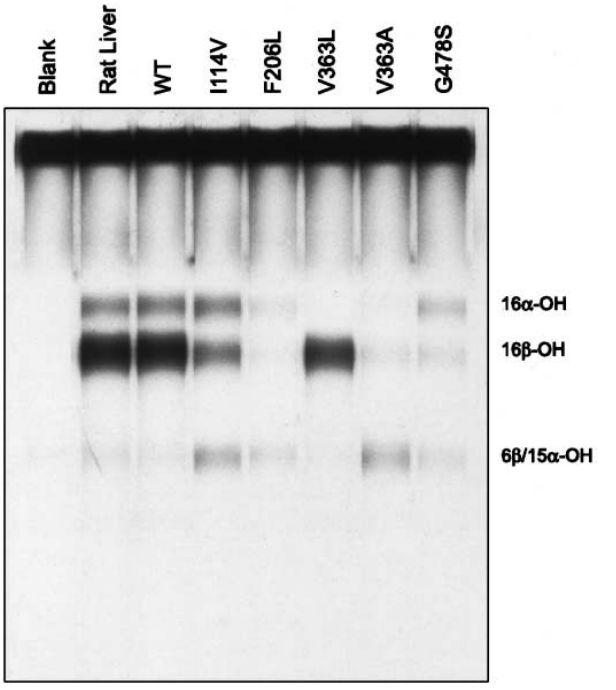

Fig. 4. Autoradiogram of androstenedione metabolites produced by hepatic and recombinant P450 2B1 and five active-site mutants. The 100-μl reaction mixture contained 5 pmol of the purified enzyme, 10 pmol of NADPH-cytochrome P450 reductase, 10 pmol of cytochrome b_5, and 25 μM substrate and proceeded for 5 min as described [2].

tion during 7-ethoxycoumarin metabolism by the wild-type and mutant enzymes are presented in Table 1. Formation of superoxide as an uncoupling product was not measured directly, due to the difficulty in making quantitative determination of this very reactive and unstable species [22]. Inclusion of superoxide dismutase yielded no increase in the amount of H_2O_2 peroxide detected, confirming that superoxide formed during the reaction was spontaneously dismutated to H_2O_2 rather than reacting with other components of the incubation mixture. Therefore, measurements of hydrogen peroxide formation served as an indicator of dissociation of oxygen from the $[FeO_2]^{2+}$-RH or $[FeO_2H]^{2+}$-RH intermediates [16,20,22]. The rates of the excess water formation presented in Table 1 were calculated from (1) the difference between the rate of NADPH oxidation and rates of hydrogen peroxide plus product formation and (2) the difference between the rate of oxygen consumption and rates of hydrogen peroxide plus product formation [16,22]. The results from both calculations were in fair agreement within experimental errors except for the mutant F206L, indicating that no major products other than 7-hydroxycoumarin were formed during the reaction.

3.3. *Uncoupling to hydrogen peroxide and water by active-site mutants*

The ratio of product formation:NADPH oxidized is presented in Table 2 in order to show the efficiency of the wild-type and mutant P450 2B1 in coupling of reducing equivalents to product. In addition to the ratios of H_2O_2 production: NADPH oxidation and H_2O formation:NADPH oxidation, the ratio of the rates of H_2O_2 production:O_2 consumption and the ratio of the rates of H_2O formation:product formation are also presented in Table 2. Use of the H_2O_2:O_2 ratio instead of the H_2O_2:NADPH ratio to analyze uncoupling at the first or second branch point shown in Fig. 1 eliminates the effect of the reducing equivalents used by the enzyme to form water at the third branch point [16]. Similarly, use of the H_2O:product ratio instead of the H_2O:NADPH ratio to assess uncoupling at the third branch point accounts for the loss of reducing equivalents to hydrogen peroxide production at the first or second branch point [16].

As shown in Table 2, the mutant I114V exhibits higher efficiency of coupling of reducing equivalents to product formation than P450 2B1 wild-type. For I114V, uncoupling to H_2O_2 production is decreased, whereas uncoupling to water formation is essentially unchanged. In contrast, the mutants V363L, F206L, V363A, and G478S all exhibit decreased efficiencies of coupling of reducing equivalents to product formation. For V363L decreased coupling efficiency is correlated

Table 1
Rates (nmol/min/nmol) determined for 7-ethoxycoumarin metabolism by P450 2B1 wild-type and five active-site mutants[a]

P450 2B1	NADPH oxidized	O_2 consumed	Product formed	H_2O_2 produced	Excess H_2O formed[b]	
					Eq. 1	Eq. 2
Wild-type	42.4 ± 3.1	34.0 ± 0.9	5.0 ± 0.2	18.6 ± 1.7	18.8 ± 1.8	20.7 ± 3.5
I114V	25.4 ± 0.8	19.1 ± 1.0	4.2 ± 0.2	6.9 ± 0.5	14.3 ± 1.0	16.1 ± 1.4
F206L	21.3 ± 0.03	10.4 ± 1.2	0.77 ± 0.06	4.8 ± 1.2	16.3 ± 0.4	11.0 ± 1.5
V363A	20.3 ± 0.5	11.8 ± 0.5	0.33 ± 0.05	3.6 ± 0.3	16.4 ± 0.5	15.6 ± 1.4
V363L	36.5 ± 0.4	35.4 ± 0.7	2.98 ± 0.07	28.0 ± 0.9	5.3 ± 1.3	8.5 ± 1.9
G478S	16.9 ± 0.7	10.9 ± 1.5	0.28 ± 0.04	6.4 ± 0.4	10.3 ± 1.1	8.5 ± 2.8

[a]The means and standard deviations were calculated from three independent experiments performed with 0.1 μM reconstituted P450 incubated for 10 min at 37°C.
[b]Eq. 1: H_2O = NADPH − H_2O_2 − product. Eq. 2: $H_2O = 2(O_2 - H_2O_2 - \text{product})$.

Table 2
Effect of active-site mutations on coupling to product formation and uncoupling to hydrogen peroxide and water formation

P450 2B1	Product[a]	H_2O_2[a]	H_2O_2[b]	H_2O[a]	H_2O[c,d]
Wild-type	0.12	0.44	0.55	0.44	3.7
I114V	0.16	0.27	0.36	0.56	3.5
V363L	0.082	0.77	0.80	0.15	1.8
F206L	0.034	0.20	0.40	0.77	23
V363A	0.016	0.18	0.31	0.80	50
G478S	0.016	0.38	0.59	0.61	38

[a]Expressed as ratios of product:NADPH, H_2O_2:NADPH, and H_2O:NADPH.
[b]Expressed as ratio of H_2O_2:O_2.
[c]Expressed as ratio of H_2O:product.
[d]Excess H_2O formation used in calculation of H_2O:product ratio was determined from Eq. 1 in Table 1. Excess H_2O formation may also be calculated from NADPH and O_2 consumption using $H_2O = 2(NADPH-O_2)$, the result of which is independent of product formed during the reaction. According to this latter calculation, the H_2O:product ratios of the enzymes in the same order as listed in the table are 3.4, 3.0, 0.7, 30, 50, and 43, respectively.

with increased uncoupling to H_2O_2. This leads to less $[FeO]^{3+}$-RH intermediate formation and consequently less product formation. At the third branch point shown in Fig. 1, however, the putative $[FeO]^{3+}$-RH intermediate of V363L substantially favors product formation. For mutants F206L, V363A, and G478S, decreased efficiencies of coupling of reducing equivalents to product formation are correlated with significantly increased uncoupling to water formation at the level of the putative $[FeO]^{3+}$-RH intermediate. Studies with P450 101 have shown that water formation is inhibited when the bound molecule is tightly packed into the active site [29]. A change from Ala to Val or from Val to Leu at position 363 increases the volume of the aliphatic side chain and presumably causes 7-ethoxycoumarin to be more tightly packed in the active pocket. The results obtained with mutants V363A and V363L indeed show that uncoupling to water formation decreases with an increase in the volume of the aliphatic side chain. Increased uncoupling to water for F206L and G478S, however, implies that factors other than volume of the side chain may also affect the complementarity between bound substrate and the active pocket. It is also inferred from the H_2O_2:O_2 ratios presented in Table 2 that an increase in volume of the side chain of residues 114 and 363 is correlated with increased uncoupling to H_2O_2. It should be noted that these particular correlations between residue volume and uncoupling may not be valid for other P450 2B enzymes or with P450 2B1 and other substrates. For example, when the volume of residue 363 increases, the monooxygenase activity can increase or decrease depending on the specific P450 2B enzyme and substrates used [5,6,11,14].

In summary, the findings from the stoichiometry of 7-ethoxycoumarin metabolism provide firm biochemical evidence that residues 206, 363, and 478 comprise part of the substrate binding site of P450 2B1. The results have important implications for engineering P450s of increased efficiency. With other substrates similar effects on uncoupling of reducing equivalents are likely to emerge for I114V.

Acknowledgements: The authors would like to thank Dr. G.D. Szklarz for docking of 7-ethoxycoumarin in the active pocket of P450 2B1. This work was supported in part by NIH Grant ES03619 and Center Grant ES06694.

References

[1] Guengerich, F.P. (1993) Drug Metab. Dispos. 21, 1–6.
[2] Kedzie, K.M., Balfour, C.A., Escobar, G.Y., Grimm, S.W., He, Y.A., Pepperl, D.J., Regan, J.W., Stevens, J.C. and Halpert, J.R. (1991) J. Biol. Chem. 266, 22515–22521.
[3] He, Y.A., Balfour, C.A., Kedzie, K.M. and Halpert, J.R. (1992) Biochemistry 31, 9220–9226.
[4] Halpert, J.R. and He, Y.A. (1993) J. Biol. Chem. 268, 4453–4457.
[5] He, Y.A., Luo, Z., Klekotka, P.A., Burnett, V.L. and Halpert, J.R. (1994) Biochemistry 33, 4419–4424.
[6] He, Y.Q., He, Y.A. and Halpert, J.R. (1995) Chem. Res. Toxicol. 8, 574–579.
[7] Kedzie, K.M., Philpot, R.M. and Halpert, J.R. (1991) Arch. Biochem. Biophys. 291, 176–186.
[8] Ryan, R., Grimm, S.W., Kedzie, K.M., Halpert, J.R. and Philpot, R.M. (1993) Arch. Biochem. Biophys. 304, 454–463.
[9] Graves, P.E., Elhag, G.A., Ciaccio, P.J., Bourque, D.P. and Halpert, J.R. (1990) Arch. Biochem. Biophys. 281, 106–115.
[10] Kedzie, K.M., Grimm, S.W., Chen, F. and Halpert, J.R. (1993) Biochim. Biophys. Acta 1164, 124–132.
[11] Hasler, J.A., Harlow, G.R., Szklarz, G.D., John, G.H., Kedzie, K.M., Burnett, V.L., He, Y.A., Kaminsky, L.S. and Halpert, J.R. (1994) Mol. Pharmacol. 46, 338–345.
[12] Szklarz, G.D., He, Y.A. and Halpert, J.R. (1995) Biochemistry 34, 14312–14322.
[13] Harlow, G.R. and Halpert, J.R. (1996) Arch. Biochem. Biophys. 326, 85–91.
[14] Szklarz, G.D., He, Y.Q., Kedzie, K.M., Halpert, J.R. and Burnett, V.L. (1996) Arch. Biochem. Biophys. 327, 308–318.
[15] von Wachenfeldt, C. and Johnson, E.F. (1995) in: Cytochrome P450: Structure, Mechanism, and Biochemistry (Ortiz de Montellano, P.R., Ed.), pp. 183–223, Plenum Press, New York.
[16] Loida, P.J. and Sligar, S.G. (1993) Biochemistry 32, 11530–11538.
[17] Mueller, E.J., Loida, P.J. and Sligar, S.G. (1995) in: Cytochrome P450: Structure, Mechanism, and Biochemistry (Ortiz de Montellano, P.R., Ed.), pp. 83–124, Plenum Press, New York.
[18] Gelb, M.H., Heimbrook, D.C., Mälkönen, P. and Sligar, S.G. (1982) Biochemistry 21, 370–377.
[19] Gould, P., Gelb, M.H. and Sligar, S.G. (1981) J. Biol. Chem. 256, 6686–6691.
[20] Gorsky, L.D., Koop, D.R. and Coon, M.J. (1984) J. Biol. Chem. 259, 6812–6817.
[21] Zhukov, A. and Archakov, A. (1982) Biochem. Biophys. Res. Commun. 109, 813–818.
[22] Gruenke, L.D., Konopka, K., Cadieu, M. and Waskell, L. (1995) J. Biol. Chem. 270, 24707–24718.
[23] John, G.H., Hasler, J.A., He, Y.A. and Halpert, J.R. (1994) Arch. Biochem. Biophys. 314, 367–375.
[24] Harlow, G.R. and Halpert, J.R. (1997) J. Biol. Chem. 272, 5396–5402.
[25] Greenlee, W.F. and Poland, A. (1978) J. Pharmacol. Exp. Ther. 205, 596–605.
[26] Fatt, I. (1976) Polarographic Oxygen Sensor, Chapter 4, CRC Press, Cleveland, OH.
[27] Green, E.J. and Carritt, D.E. (1967) J. Mar. Res. 25, 140–147.
[28] Jiang, Z.Y., Woollard, A.C.S. and Wolf, S.P. (1990) FEBS Lett. 268, 69–71.
[29] Atkins, W.M. and Sligar, S.G. (1989) J. Am. Chem. Soc. 111, 2715–2717.